Non-Uniform Excitonic Charge Distribution Enhances Exciton-Phonon Coupling in ZnSe/CdSe Alloyed Quantum Dots

Ke Gong, David F. Kelley,* and Anne Myers Kelley*

Chemistry & Chemical Biology, University of California, Merced, 5200 North Lake Road, Merced, CA 95343

*Authors to whom correspondence should be addressed: dfkelley@ucmerced.edu, amkelley@ucmerced.edu

Abstract

Zinc to cadmium cation exchange of ZnSe quantum dots has been used to produce a series of alloyed $Zn_{1-x}Cd_xSe$ quantum dots. As x increases and the lowest-energy exciton shifts to the red, the peak initially broadens and then sharpens as x approaches 1. Resonance Raman spectra obtained with excitation near the lowest excitonic absorption peak show a gradual shift of the longitudinal optical phonon peak from 251 cm^{-1} in pure ZnSe to 210 cm^{-1} in nearly pure CdSe with strong broadening at intermediate compositions. The LO overtone to fundamental intensity ratio, a rough gauge of exciton-phonon coupling strength, increases considerably for intermediate compositions compared with either pure ZnSe or pure CdSe. The results indicate that partial localization of the hole in locally Cd-rich regions of the alloyed particles increases the strengths of local internal electric fields, increasing the coupling between the exciton and polar optical phonons.

Table of contents graphic

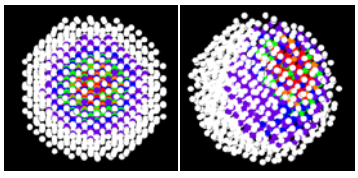

Exciton-phonon coupling (EPC) describes the change in the potential surface for nuclear motion that is caused by creation of an exciton. In polar binary semiconductors such as the Cd and Zn chalcogenides, the dominant mechanism for coupling to the optical phonons is assumed to be the so-called Fröhlich mechanism, in which the dipoles produced by the vibrating atoms interact with the local electric field of the exciton. The magnitude of the electric field is determined by the different spatial extents of the electron and hole wavefunctions. The excitonic energies and wavefunctions of quantum dots (QDs) are often described using variations on the particle-in-a-sphere effective mass approximation (EMA) model.[1-3] These models assume that the potentials that determine the wavefunctions are spherically symmetric and that the potential function is constant within areas of the same composition. As a result, the lowest-energy excitonic transition is described in terms of S functions for both the electron and the hole. Finite potentials at the boundary along with their different effective masses cause the electron and hole functions to differ slightly in their radial extent. The resulting electric field produced by creation of an electron-hole pair inside the QD is therefore spherically symmetric and relatively weak.

In the strong quantum confinement limit, the difference in the spatial extents of the electron and hole wavefunctions is expected to decrease with increasing particle size. This will decrease the magnitude of the electric field and implies that the EPC should also decrease with increasing QD size in single-component structures. Due to the difference in valence and conduction band offsets, formation of a "type 1½" or "quasi type II" structure by adding a CdS shell to a CdSe QD would be expected to greatly increase the magnitude of the electric field and strongly increase the magnitude of the EPC. However, previous experimental results contradict both expectations.[4,5] These results have led us to question some of the key assumptions of the

particle-in-a-sphere EMA model for the excitonic wavefunctions, and look more closely at the role of structural heterogeneities at smaller length scales.

We have recently shown that the exciton-phonon coupling in pure ZnSe QDs is somewhat larger than in CdSe but still in the "weak" EPC limit (Huang-Rhys factor << 1).[6] In these materials the larger anions form a relatively rigid structure through which the cations can move fairly freely at elevated temperatures. It has been shown that as a consequence, ZnSe quantum dots can be converted to alloyed $Zn_{1-x}Cd_xSe$ structures by heating in the presence of excess cadmium, while retaining the size and shape of the original structure.[7-9] The CdSe bond is considerably stronger than the ZnSe bond, so this ion exchange process is energetically favorable and proceeds to almost quantitative replacement. If the alloying process amounts to random (rather than uniform) replacement of Zn atoms by Cd atoms, then spatial fluctuations in the fraction of each type of atom will result in potentials for electron and hole motion that are non-constant from one unit cell to another and therefore no longer spherically symmetric. If the resulting spatial variations in the potential are sufficiently strong to partially localize one of the carriers (presumably the hole because of its much larger effective mass), then there will be enhancement of the local electric fields inside the QD and we might expect stronger EPC in the alloys.

In order to test this hypothesis, we employed the general synthetic methods of ref. 8 to create alloyed $Zn_{1-x}Cd_xSe$ QDs. Figure 1 (left) shows the absorption spectra of the original ZnSe sample and aliquots taken at various times during cation exchange. As zinc is replaced by cadmium, the absorption spectrum initially shifts to the red and also broadens considerably. As the exchange proceeds, the spectrum continues to shift to the red and starts to sharpen somewhat.

Figure 1 (right) shows the normalized photoluminescence spectra of the five longest-wavelength absorbing samples. The four bluer-absorbing samples exhibited very weak photoluminescence.

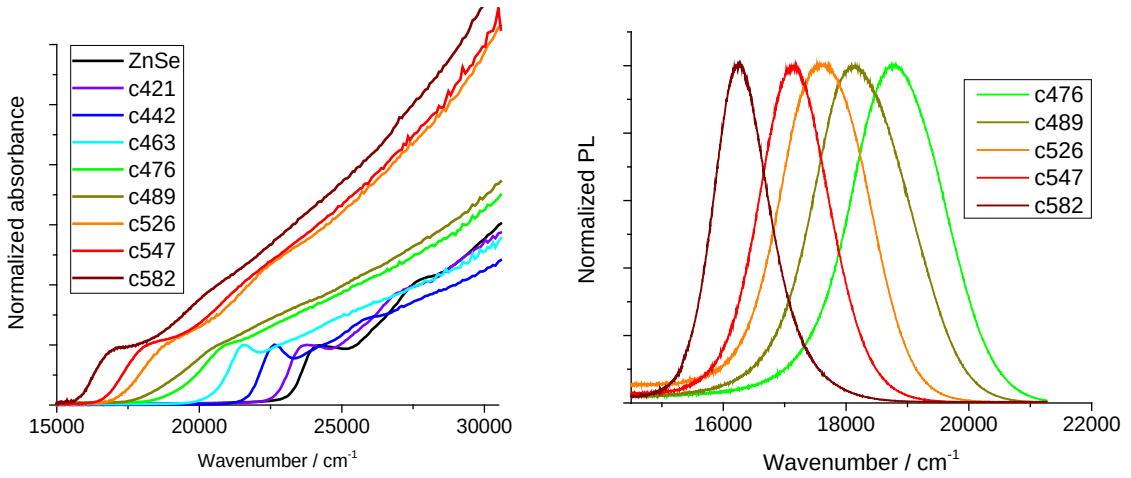

Figure 1. Left: normalized absorption spectra of original ZnSe QDs absorbing at 413 nm, and aliquots taken in the course of the Zn to Cd cation exchange. Spectra are labeled by approximate absorption maximum. Right: normalized photoluminescence spectra of the five longest-wavelength absorbing samples.

The QDs are approximately spherical with diameters of 4.5 ± 0.2 nm for pure ZnSe (determined from the absorption maximum[6]), 4.6 ± 0.5 nm for c489 (from TEM images, see Supporting Information), and 5.2 ± 0.6 nm for c582 (from TEM). The Cd fraction was determined from the absorption maxima as described in the Supporting Information. With the assumption of random alloy formation, the fraction of cadmium is calculated to be approximately 0.04, 0.14, 0.23, 0.30, 0.36, 0.53, 0.63, and 0.81 for samples c421 through c582, respectively, in Figure 1. We note that cation exchange was performed at 220 °C followed by heating to 230 °C, which is slightly lower than the temperature needed for complete exchange. These cation exchange conditions were chosen because ref. 8 reports that at 250 °C, the particles increase in size and become irregular in shape. Furthermore, we find that at 250 °C the cation exchange reaction is too fast to allow aliquots to be taken at multiple stages in the exchange. Ref. 8 shows that cation exchange at 220 °C results in particles that are close to, but not entirely, fully alloyed.

Thus, our particles are probably better described as core/shells with a highly interdiffused interface rather than homogeneous random alloys. EMA calculations similar to those described in ref. 10 indicate that incomplete interdiffusion of the metal atoms will result in slightly larger estimates of the cadmium fractions in the alloyed particles than given above. We emphasize that the exact amount of exchange in each of these samples and exact radial composition profiles are unimportant in the analysis of the present results. The important point is that any randomly alloyed regions will contain regions of locally high Cd concentration which will localize the holes and cause increased EPC. Calculations on a core/shell structure with a significantly diffused interface show that it makes little difference whether the alloying is complete or whether there remains a radial composition gradient (see Supporting Information).

Figure 2 (left) displays the resonance Raman spectra, excited near the lowest-energy excitonic absorption maximum, of five of the samples. The pure ZnSe QDs show a strong peak at 251 cm^{-1} which corresponds to the longitudinal optical (LO) phonon, plus weaker peaks near 500 and 750 cm^{-1} from the first and second overtones. As the zinc to cadmium exchange proceeds, both the overtone and the fundamental develop rather complicated multi-peaked shapes, shift to lower frequencies, and broaden considerably. In the final sample, which is mostly CdSe, the fundamental frequency is 210 cm^{-1}, just a few wavenumbers higher than in a pure CdSe QD of the same size. The intensity in the broad LO overtone range relative to the fundamental increases dramatically between pure ZnSe and the roughly equal mixture of zinc and cadmium, then decreases as the composition becomes mostly CdSe. Figure 2 (right) plots the average LO phonon frequency and the first overtone to fundamental intensity ratio as a function of the lowest excitonic absorption wavelength.

These results are qualitatively reproducible when starting from different original ZnSe QDs. The Supporting Information shows similar results obtained starting from smaller ZnSe QDs.

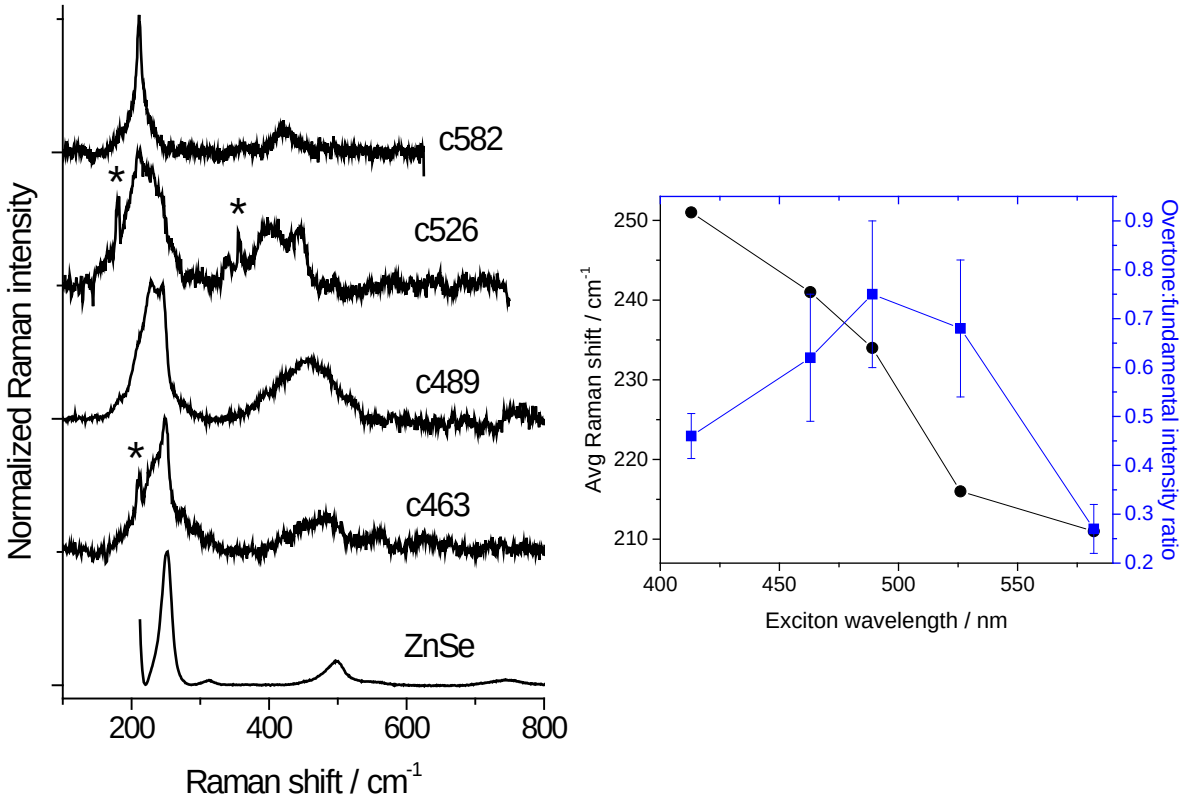

Figure 2. Left: Resonance Raman spectra of five samples from Fig. 1. Fluorescence backgrounds have been subtracted and spectra are scaled and offset. Asterisks mark artifacts from small pixel-to-pixel variations in light sensitivity. Excitation wavelengths are, from bottom to top, 417, 458, 477, 515, and 561 nm. Right: Average Raman frequency and Raman overtone to fundamental intensity ratio.

The shift of the lowest excitonic transition to longer wavelengths and of the LO phonon to lower frequencies as zinc is replaced by cadmium are expected given the nearly 1 eV smaller bulk band gap for CdSe than ZnSe and the ~40 cm^{-1} lower LO phonon frequency in bulk CdSe. The increase in breadth of the absorption, photoluminescence, and Raman spectra for intermediate compositions is attributed at least in part to inhomogeneous broadening resulting from the existence of an ensemble of QDs having different compositions. Some of the increased absorption width at intermediate compositions may also arise from a reduction in the symmetry

of the excitonic wavefunctions induced by the "lumpiness" in the potential functions for electrons and/or holes in the alloyed structures. The loss of spherical symmetry mixes basis functions of different angular momentum and makes transitions allowed to excitonic states such as "$1S_e1P_h$" (the S and P labels now being only approximate) in addition to those that are allowed in the spherically symmetric case (*e.g.* $1S_e1S_h$, $1P_e1P_h$). However, this mechanism should have little effect on the thermally equilibrated photoluminescence, which also narrows considerably as x approaches 1. The increased exciton-phonon coupling evidenced by the increased Raman overtone intensity in the intermediate composition samples should also contribute to the increased breadth of the electronic spectra although this is unlikely to be the major mechanism.

It is important to recognize that if the substitution of cadmium for zinc is truly random, then statistical variations in a structure having a nominal composition $Zn_{0.5}Cd_{0.5}Se$ will result in some regions that are cadmium-rich and other regions that are zinc-rich. The cadmium-rich regions will have a lower potential energy for both electrons and holes, tending to localize both in these regions. This effect should be greater for the hole because of its much larger effective mass. The large effective mass implies that relatively shallow potential wells may be quite effective at localizing the holes. The results of ref. 11 also suggest that holes are relatively easy to localize.

In order to further explore the effects of zinc to cadmium exchange on both the electronic and vibrational spectra, calculations were carried out on $Zn_{1-x}Cd_xSe$ quantum dots of ~3.8 nm diameter at compositions of x = 0, 0.25, 0.5, 0.75, and 0.95. Electron and hole EMA wavefunctions were calculated for pure and random alloyed particles at these compositions. While the nominal effective masses obtained from bulk measurements are only about a factor of four larger for holes than for electrons in both CdSe and ZnSe, a considerably larger hole

effective mass is needed to reproduce the $1S_e1S_{3/2}$ to $1S_e2S_{3/2}$ spectroscopic splittings in CdSe QDs when a simple two-band model is employed[4] rather than more complicated treatments that include valence band mixing.[3] Details of the calculations are given in the Supporting Information. Figure 3 shows the distribution of hole and electron densities for the pure ZnSe structure and for a nearly equal mixture of Cd and Zn ($Zn_{257}Cd_{250}Se_{507}$). For the pure structure, both the hole and the electron are spherically symmetric and have nearly complete overlap, resulting in very small internal electric fields. For the 50:50 alloy, the wavefunctions are not spherically symmetric and the hole function is much more localized than the electron, resulting in a high degree of charge separation and large internal electric fields. The asymmetry of the hole wavefunction nearly vanishes if a hole effective mass of 0.5, roughly the average bulk value, is used instead of the spectroscopically consistent value of 2.0. Figure 4 shows calculated resonance Raman spectra and the Huang-Rhys parameter and peak Raman frequency. The Huang-Rhys parameter is calculated to be essentially zero for pure ZnSe because these calculations do not include the penetration of the electron wavefunction outside the particle. As such, these simple simulations are not expected to be quantitative. However, the calculations do capture the effect of a large increase in exciton-phonon coupling at the 50-50 mixture and a rapid falloff for the mostly-Cd or mostly-Zn structures. The applicability of bulk band offsets to regions of just one or a few Cd atoms is highly questionable, as is the assumption that the replacement of Zn by Cd is truly random. The expansion of the lattice required to accommodate one Cd atom probably makes it easier for nearby Zn atoms to exchange, making a truly random alloy energetically unfavorable. However, these simulations do qualitatively capture the experimental behavior displayed in Figure 2.

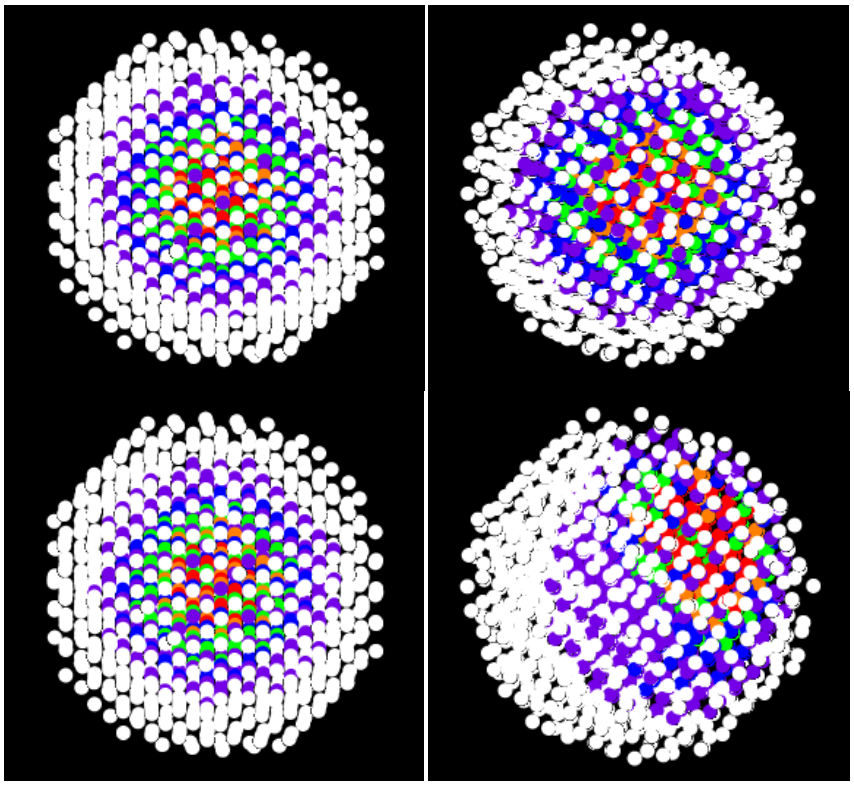

Figure 3. Calculated distribution of electron (top) and hole (bottom) densities for pure ZnSe (left) and for a 50:50 ZnSe/CdSe alloy (right). White, violet, blue, green, orange, and red correspond to increasing densities relative to the maximum density for that structure.

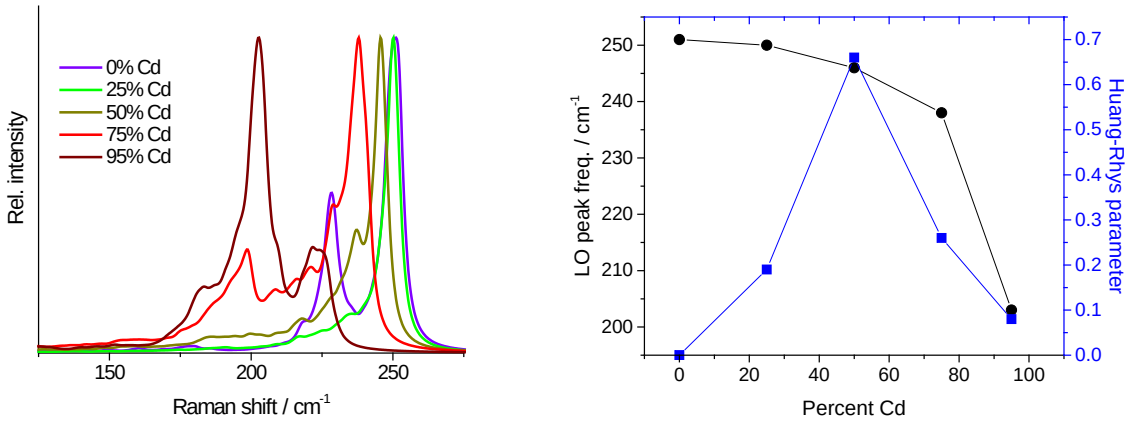

Figure 4. Left: calculated resonance Raman spectra, scaled to a common maximum, for ZnSe/CdSe alloys with the indicated fraction of Cd. Right: calculated Huang-Rhys parameters and LO phonon peak frequencies.

The overtone to fundamental resonance Raman intensity ratio is often used as a proxy for exciton-phonon coupling strength or the Huang-Rhys parameter, S. This ratio also depends on the degree of detuning from electronic resonance, interferences among contributions from different near-resonant excited states, and the magnitude of the electronic homogeneous broadening.[12] We have chosen the excitation to be near the first excitonic absorption maximum to minimize variations in the first two factors from one sample to another. The electronic homogeneous width is not expected to vary greatly, so we believe it is safe to conclude that stronger overtones indicate stronger exciton-phonon coupling.

Localization of excitons resulting from random potential fluctuations is well known in bulk-scale semiconductor alloys.[13-15] However, disorder-induced localization in the bulk does not necessarily transfer to a quantum dot system in which the quantum confinement energy is significant. Our results indicate that some localization does occur, at least enough to break the near-spherical symmetry of the original QD and turn on new channels for coupling to polar phonons. The calculations of Fig. 3 indicate that it is primarily the hole that becomes localized in these random alloys. Those calculations assume that the valence band and conduction band offsets between ZnSe and CdSe are 0.3 and 0.7 eV, respectively (ZnSe higher in both cases), consistent with the offsets reported in ref. 16. Other reports place the valence bands closer in energy,[17] but even a small energy difference will lead to some localization if the effective mass of the hole is as large as implied by the spectroscopy of CdSe QDs.[4] We suggest that the weak exciton-phonon coupling in pure CdSe QDs (Huang-Rhys parameter $S \sim 0.2$) arises largely from partial localization of the hole wavefunctions because of irregularities in the crystal structure or surface charges, explaining why the Huang-Rhys parameter is nearly independent of QD size and of electron delocalization into a CdS shell.[5]

Time-resolved techniques have been utilized to probe dynamic localization of holes following excitation to a delocalized state in many semiconductor nanostructures. In this work, we use optical absorption and resonance Raman spectroscopies to conclude that in a randomly alloyed CdSe/ZnSe QD the initially formed exciton, prior to thermal equilibration or any significant nuclear reorganization, already has the hole considerably localized. Our work provides a complementary view of the roles of quantum confinement and energetic disorder on charge-carrier localization.

Experimental section

ZnSe QDs were synthesized as described in ref. 6 and ZnSe/CdSe alloyed QDs were synthesized following the procedure described in ref. 8 and detailed in the Supporting Information. Aliquots of the alloyed QDs were dissolved in chloroform and washed several times by precipitation with methanol, centrifuged, and redissolved in chloroform containing methyl viologen and hexadecanethiol as fluorescence quenchers. The QDs were then deposited as thin films on aluminum substrates for Raman spectroscopy. Resonance Raman spectra were obtained using the apparatus and general methods described previously.[4,6,18] The resonance Raman spectrum of each sample was obtained using an excitation wavelength that was close to the lowest excitonic absorption maximum in order for the overtone to fundamental intensity ratios to accurately reflect the exciton-phonon coupling in this transition. The laser was focused onto the sample and the Raman scattering was collected with a 10x microscope objective with an average power at the sample of ~0.2 mW. The sample was translated continuously to avoid local heating or photodamage. Even with both electron and hole quenchers added, excitation near the lowest excitonic absorption maximum generated significant fluorescence backgrounds in all

samples. A background was removed using Origin Pro 2015 and the Raman peak areas were determined by fitting regions of the subtracted spectrum to a sum of peaks in Grams AI. Examples of original unsubtracted spectra are shown in the Supporting Information.

This work was supported by NSF grant CHE-1506803. The TEM images shown in the Supporting Information were obtained with the assistance of Gary Beane and David Morgan at the UC Merced Imaging and Microscopy Facility.

Supporting Information. Synthetic methods; details of the calculations used to produce Figs. 3 and 4; data corresponding to Figs. 1-2 for a smaller initial size of ZnSe QDs; sample Raman spectra before fluorescence subtraction; TEM images; calculation of cadmium fraction in samples; calculations of electron and hole wavefunctions for diffuse interface core/shell QDs. This material is available free of charge via the Internet at http://pubs.acs.org.

References

1. Efros, A. L.; Rosen, M.; Kuno, M.; Nirmal, M.; Norris, D. J.; Bawendi, M. Band-Edge Exciton in Quantum Dots of Semiconductors with a Degenerate Valence Band: Dark and Bright Exciton States. *Phys. Rev. B* **1996**, *54*, 4843-4856.

2. Kelley, A. M. Electron-Phonon Coupling in CdSe Nanocrystals from an Atomistic Phonon Model. *ACS Nano* **2011**, *5*, 5254-5262.

3. Norris, D. J.; Bawendi, M. G. Measurement and Assignment of the Size-Dependent Optical Spectrum in CdSe Quantum Dots. *Phys. Rev. B* **1996**, *53*, 16338-16346.

4. Lin, C.; Gong, K.; Kelley, D. F.; Kelley, A. M. Size Dependent Exciton-Phonon Coupling in CdSe Nanocrystals through Resonance Raman Excitation Profile Analysis. *J. Phys. Chem. C* **2015**, *119*, 7491-7498.

5. Lin, C.; Gong, K.; Kelley, D. F.; Kelley, A. M. Electron-Phonon Coupling in CdSe/CdS Core-Shell Quantum Dots. *ACS Nano* **2015**, *9*, 8131-8141.

6. Gong, K.; Kelley, D. F.; Kelley, A. M. Resonance Raman Spectroscopy and Electron-Phonon Coupling in Zinc Selenide Quantum Dots. *J. Phys. Chem. C* **2016**, *120*, 29533-29539.

7. Zhong, X.; Han, M.; Dong, Z.; White, T. J.; Knoll, W. Composition-Tunable $Zn_xCd_{1-x}Se$ Nanocrystals with High Luminescence and Stability. *J. Am. Chem. Soc.* **2003**, *125*, 8589-8594.

8. Groeneveld, E.; Witteman, L.; Lefferts, M.; Ke, X.; Bals, S.; Van Tendeloo, G.; de Mello Donega, C. Tailoring ZnSe-CdSe Colloidal Quantum Dots Via Cation Exchange: From Core/Shell to Alloy Nanocrystals. *ACS Nano* **2013**, *7*, 7913-7930.

9. De Trizio, L.; Manna, L. Forging Colloidal Nanostructures Via Cation Exchange Reactions. *Chem. Rev.* **2016**, *116*, 10852-10887.

10. Beane, G. A.; Gong, K.; Kelley, D. F. Auger and Carrier Trapping Dynamics in Core/Shell Quantum Dots Having Sharp and Alloyed Interfaces. *ACS Nano* **2016**, *10*, 3755-3765.

11. Pinchetti, V.; Meinardi, F.; Camellini, A.; Sirigu, G.; Christodoulou, S.; Bae, W. K.; De Donato, F.; Manna, L.; Zavelani-Rossi, M.; Moreels, I.; Klimov, V. I.; Brovelli, S. Effect of Core/Shell Interface on Carrier Dynamics and Optical Gain Properties of Dual-Color Emitting CdSe/CdS Nanocrystals. *ACS Nano* **2016**, *10*, 6877−6887.

12. Kelley, A. M. Resonance Raman Overtone Intensities and Electron-Phonon Coupling Strengths in Semiconductor Nanocrystals. *J. Phys. Chem. A* **2013**, *117*, 6143-6149.

13. Sugisaki, M.; Ren, H.-W.; Nishi, K.; Sugou, S.; Masumoto, Y. Excitons at a Single Localized Center Induced by a Natural Composition Modulation in Bulk $Ga_{0.5}In_{0.5}P$. *Phys. Rev. B* **2000**, *61*, 16040-16044.

14. Shevel, S.; Euteneuer, A.; Hellmann, R.; Gobel, E. O.; Vozny, V.; Vytrykhivsky, M.; Petri, W.; Klingshirn, C. Effect of Disorder on Exciton Dynamics in Cation-Substituted $Zn_xCd_{1-x}S$ Mixed Crystals. *Phys. Stat. Sol. B* **1998**, *205*, 667-681.

15. Ouadjaout, D.; Marfaing, Y. Localized Excitons in II-VI Semiconductor Alloys: Density-of-States Model and Photoluminescence Line-Shape Analysis. *Phys. Rev. B* **1990**, *41*, 12096-12105.

16. Rangel-Kuoppa, V.-T. Determination of Conduction Band Offset between Strained CdSe and ZnSe Layers Using Deep Level Transient Spectroscopy. *Appl. Phys. Lett.* **2012**, *100*, 252110.

17. Hinuma, Y.; Gruneis, A.; Kresse, G.; Oba, F. Band Alignment of Semiconductors from Density-Functional Theory and Many-Body Perturbation Theory. *Phys. Rev. B* **2014**, *90*, 15405.

18. Baker, J. A.; Kelley, D. F.; Kelley, A. M. Resonance Raman and Photoluminescence Excitation Profiles and Excited-State Dynamics in CdSe Nanocrystals. *J. Chem. Phys.* **2013**, *139*, 024702.